GRINDING MECHANICS AND ADVANCES - A REVIEW

P. V. Vinay[1*], C. S. Rao[2]

[1]Department of Mechanical Engineering,
GVP College for Degree and PG Courses (Technical Campus),
Rushikonda, Visakhapatnam, India

[2]Department of Mechanical Engineering,
Andhra University College of Engineering (A),
Visakhapatnam, India

ABSTRACT

The process of grinding involves the interaction between the grain and bond of the wheel to the workpiece whose properties will affect the output as the process happens. The properties of wheel which influence the creation of the ground surface are identified and categorised as length of chip, number of cutting points, chip thickness, surface roughness, force mechanics, abrasion mechanics, and fracture toughness. These afore mentioned properties are reviewed with an intention to delve upon the factors which influence the process of grinding with an overview of the underlying mechanics involved in the process which govern the outcome such as surface roughness, quality of the surface with no subsurface imperfections and minimal energy requirements.

KEYWORDS*: Grinding mechanics; Length of chip; Abrasive wear; Surface roughness; Force mechanics; Chip thickness*

1.0 INTRODUCTION

Grinding is a complex abrasive cutting process where machining happens with geometrically unspecified cutting edges. Grinding interface involves material removal by contact, between the grinding wheel and a random structured surface of the workpiece. Each grain removes a chip from the surface of the workpiece material and generates a surface with a certain roughness. Grinding also refers to material removal by individual grains whose cutting edge is bounded by force and a path. The interface friction conditions, the flow characteristics of the material and the cutting speed have a significant influence on chip formation. A consistent cutting mechanism description therefore

* Corresponding author email: vpragada@yahoo.com

comprises complex penetration relationships between two hard materials, elasto-plastic mechanics and aspects of tribology, which all influence the kinematics and contact condition.

2.0 LENGTH OF CHIP

The surge of grinding as a machining process has led to the mechanics behind the process researched upon to generate enough idea about this unpredictable and elusive but much used finishing process. This started with the formulation of undeformed chip thickness and average chip length which play a major role in finding the forces acting on the tool and the workpiece (Hahn, 1962).

The average chip length l_c is given as

$$l_c = \sqrt{f d_t} \tag{1}$$

The average metal removal rate $Z_w = f a_p v_w$

where

f is depth of cut
d_t is the grinding wheel diameter
a_p is the back engagement(width)
v_w is the surface speed of the workpiece

The maximum undeformed chip thickness enhances the maximum force acting on each active grain and also the self-sharpening process of the grains and the wheel will tend to behave softer if v_w is decreased or v_t is increased (Shaw, 1972).

$$t^2 c_{max} = \frac{K v_w}{v_t} \sqrt{f} \tag{2}$$

where

$$K = \frac{6}{C_g r_g \sqrt{d_t}} \tag{3}$$

C_g is the number of active grains
r_g is the grain aspect ratio
d_t is the grinding wheel diameter in mm

v_w is the work surface speed in mm/sec
v_t is the grinding wheel surface speed in mm/sec
f is the depth of cut in mm

For cylindrical grinding the maximum undeformed chip thickness is given as

$$t_{cmax} = \frac{v_w}{C_g v_t}\sqrt{\frac{2d(R_p+R_w)}{R_p R_w}} \tag{4}$$

where

R_p is workpiece radius
R_w is wheel radius
d is the radial depth of cut
C_g is the number of active grits
v_t is the grinding wheel surface speed
v_w is the work surface speed

Contact length has been measured using thermocouples (Verkerk, 1975), explosives (Brown and Watson, 1977) and it was measured reliably and experimentally shown by (Zhang et al., 1993) as a relation with the elastic modulus of the wheel and found that the length at which the forces are exerted is at the middle of the geometrical length which is 0.7 times theoretical length and which in turn is almost equal to the experimental length. Smaller chip thickness corresponds to smaller pressure value (Lindsay, (1975), p42-60). The deformation of workpiece and wheel reduce the depth of cut was found that for a specific situation the value is to be 0.938 times the nominal depth of cut.

A new relation for chip length was proposed by (Zhang et al., 1993) and it is compared with the available models and have deduced that this formulation for chip length is reasonably good and given as

$$l_c = R_d arccos\left(1 - \frac{d_c}{R_d}\right) \tag{5}$$

where equivalent wheel radius after deformation

$$R_d = R_0\left(1 + \zeta\frac{(1-\nu_s^2)F_n'}{E_s d_c}\right) \tag{6}$$

R_0 is the equivalent wheel radius before deformation
ζ = constant that can be determined by a set of measured data for a class of grinding operations
v_s is the poisson's ratio of the wheel
d_c is the real depth of wheel cut
E_s is the elastic modulus of the grinding wheel
F_n' is the normal grinding load per unit wheel width

An approximate model for the determination of chip length can be held viable only when $1 \leq \frac{L_c}{L_g} \leq N$ where L_c is modified contact length, L_g is geometrical contact length and N is a finite constant. And a further assertion given as the macro deformation of the wheel workpiece system is one of the most important factors which contribute to the variation of contact length during grinding.

Chip length has been represented by (Rowe, Qi et al., 1993, 1993a, 1994) as a combination of the deformation contact length l_f and the geometric contact length l_g as

$$l_c^2 = l_f^2 + l_g^2 \tag{7}$$

Contact length in grinding is dependent on the effects of elastic/plastic deformation between the rough surface of the grinding wheel and the surface of the workpiece, the expression of deformation contact length relative to rough surfaces in contact was given as

$$l_c = [R_r^2 * 8 * F_n' * (K_s + K_w) * d_e + a_e d_e]^{0.5} \tag{8}$$

where

$$K_s = \frac{(1-v_s^2)}{\pi E_s}, K_w = \frac{(1-v_w^2)}{\pi E_w} \tag{9}$$

E_s , E_w are moduli of elasticity of grinding wheel and workpiece (kN/ mm^2)
v_s,v_w are the poisson ratios' of the grinding wheel and workpiece
F_n' is specific normal force (N)
a_e is real depth of cut (mm)
d_e is equivalent diameter of the grinding wheel (mm)
R_r is the roughness factor

An applied power source method to measure the real contact length was used by (Qi et al., 1997). The experimental measurement of contact length shows that the real contact length is larger than the geometrical length and the ratio of the previous two lengths as reported by (Makino et al., 1966) which suggests for conventional grinding operations the real contact length may be approximately twice the geometric length and (Maris, 1977) are not approximately constant. Further the authors experimented with EN9 steel ground using a CBN grinding wheel and concluded that the contact length ratio is insensitive to depth of cut but it increases from approximately 2.2 for dry grinding to 2.8 for wet grinding which points out that the usage of coolant increases the contact length. With the consideration of coolant the distribution of normal pressure changed over the contact area due to hydrodynamic action which led to the flattening the part of the grinding wheel in contact with the workpiece. It was also pointed out that the table speed has changed the contact length which in turn increased the material removal rate and subsequently the normal force. The length of grinding harder material as cast iron when compared with EN9 steel showed that EN9 had a grinding length twice that of grinding cast iron, this phenomenon cannot be explained by Hertz contact theory. A decrease in roughness factor R_r will result in a decrease of the real contact length according to equation (8). This length of chip has significance when viewed with the number of cutting points that effect the material removal from the workpiece during grinding.

3.0 NUMBER OF CUTTING POINTS AND CHIP THICKNESS

The number of contacting or cutting points in a grinding wheel plays an important role on the mechanics of grinding. Not all abrasive grains on the surface of a grinding wheel participate in the grinding process. Some may cut, others may rub or plough and a large number may not be doing anything at all. The grinding wheel specifications like the variety of abrasive, grain size, type of bond, hardness, structure of the wheel, the wheel and workpiece interactions, grinding conditions such as wheel speed, work speed, depth of cut, forces, grinding fluid, etc. used, the stiffness and accuracy of the machine tool all play an important role.

Estimation of the number of apparent contact points by rolling the grinding wheel under its own weight on soot covered glass plate was done by (Backer et al., 1952). The image is photographically enlarged and projected on to a screen. The number of cutting points per unit area

is determined by counting the number of spots. It was reported that for a 46-grit alumina wheel, the number of cutting grains per unit area, n to be 299 grains/cm^2 or 1930 grains/in^2. Further it was pointed out that the count is actually an estimate of the number of peaks of the abrasive grits on the wheel surface that have penetrated the carbon film and not necessarily the number of actual contacting or cutting grains per unit area.

A technique of rolling the grinding wheel over a piece of Sanborn recording paper and counting the number of contacts of a cut-off wheel was done by (Shaw et al., 1967). Another technique of wrapping a thin steel band (0.010 in. thick razor blade stock) around the periphery of the grinding wheel to observe the projected image on to a screen to count the contacting points was also discussed.

A dynamic method was developed by (Brecker and Shaw, 1974) unlike the above ones to determine the effective number of cutting points on the surface of a grinding wheel. It employs a thin workpiece mounted on a special piezoelectric dynamometer of very high natural frequency of response to measure the instantaneous forces. The workpiece is so thin that only one grain is assumed to be in contact at a given time. The number of chips produced in a given time is determined by counting the number of force peaks. While there are some limitations associated with this technique, it is by far the most accurate method for obtaining the number of cutting points under dynamic conditions.

The grinding process of finish and cut-off grinding was analysed using probability statistics by (Hou and Komanduri, 2003) and experimentally found that the percentage of grains that participate in actual machining are 0.15 in finish and 1.8 in cut-off grinding, the remaining grains rub or plough the workpiece material.

The specific energy can be calculated by using simple mechanics of grinding. Figure 1 shows the grinding wheel mechanism at the workpiece interaction in order to derive the specific energy in the grinding process.

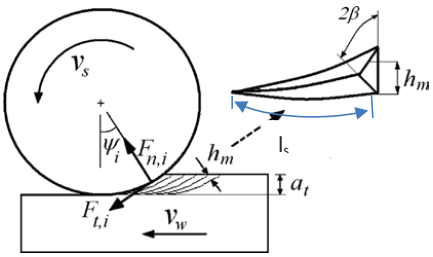

Figure 1. Chip thickness in grinding (Mahdi and Zhang, 1999)

The total specific energy, u generated by the grinding process as postulated by (Malkin, 1989) is

$$u = u_{chip} + u_{plough} + u_{rub} \tag{10}$$

and the specific energy of the chip being the main concern is given as

$$u = \frac{W_p}{Q_w} = \frac{F_t * v_s}{a_t * b * v_w} \tag{11}$$

where

W_p is the grinding power
Q_w is the volumetric material removal rate
F_t is the tangential grinding force
a_t is the true depth of cut
b is the width of grinding
v_s is the wheel speed
v_w is the workpiece speed

The specific energy is related to the maximum undeformed chip thickness h_m as given by (Malkin, 1989)

$$h_m = \left[\frac{3}{Ctan\beta}\left(\frac{v_w}{v_s}\right)\left(\frac{a_t}{d_s}\right)^{1/2}\right]^{1/2} \tag{12}$$

where

d_s is the wheel diameter
C is active grits per unit area of wheel surface
β is the semi-included angle of the chip cross-section which can be taken as triangular as shown in Figure 1 and taken as 60^0 for calculation of *hm* by (Malkin, 1989).

The grinding process can quantitatively be accounted for the magnitude of the specific energy and its dependence on the process parameters. The grinding energy is apparently expended mainly by ploughing. This suggests a need for a ductile ploughing model to account for the energy used. The analysis of the ploughing behaviour for tools having triangular cross-sections gives results which are generally dependent on the semi-included angle β and it is independent of the ploughing depth (Vathaire et al., 1981; Gilormini and Felder, 1983; Torrence, 1996). However a more complex analysis for a trapezoidal cross-section square based pyramidal tool conducted by (Abebe and Appl, 1988) indicates that the specific energy should decrease with a larger ploughing depth. From experimental measurements of the grinding forces and power, it has been found that the specific grinding energy increases as the undeformed chip thickness is decreased (Malkin, 1989). The inverse relationship between specific energy and undeformed chip thickness is often referred to as the 'size effect'. (Hwang and Malkin, 1999) modified the upper bound solution of (Vathaire et al., 1981) by including the effect of rounding the tip of the triangular-shaped cutting tool. In this approach, the upper bound solution matches the experimental measurements of the grinding specific energy. The shape of the cross-sectional cutting profile was then calculated. The results showed that rounding the tip of a cutting tool can account for an increase in specific energy with smaller undeformed chip thickness. The undeformed chip thickness was later modified as the β cannot be predicted accurately by the pyramidal tool relationship as given by (Suh, (1986), chap7). (Hwang and Malkin, 1999) modified the undeformed chip thickness, taking into account that the tip be taken as round to decrease the specific energy which is stated by (Vathaire et al., 1981) as

$$\frac{u}{k} = \frac{A_s}{h_m} + B_s \tag{13}$$

where

A_s and B_s are constants found out from experiment using least squares fitting method.

$$h_m = \frac{A_f}{\sqrt{tan\beta}}(h_m tan\omega)^2 \tag{14}$$

An earlier version of the upper bound method developed by the same researchers was extended by (Azarkhin et al., 1996) to find the configuration of a stress-free surface, to a more complicated kinematic

field and geometry of indenter. The purpose of this generalization was twofold. First, it gave more flexibility in using the results of the friction study for a wider set of problems, including the case of interfering asperities. Numerical results for a row of asperities with different degrees of penetration up to full embedment were presented. Second, the algorithm was used to model the indentation of a rigid wheel pressed into softer rigid-perfectly plastic material, and then dragged through it, leaving a groove behind. The wheel may be prevented from rotation or may be torque free. Key issues to be determined from the analysis include an evaluation of local pressures, sliding speeds, development of plastic deformation and exposure of nascent material. Their numerical results have shown that for a certain range of parameters, the ratio of ploughing force to vertical force may decrease as the local adhesion increases. The effect of the prior said parameters has a profound influence on the surface roughness generated on the workpiece.

4.0 SURFACE ROUGHNESS

The ploughing of workpiece with a pyramidal tool of square base if used as done by (Gilormini and Felder, 1983) is shown in the Figure 2 which shows different heights as well as the angles during grinding with a single point pyramidal grain.

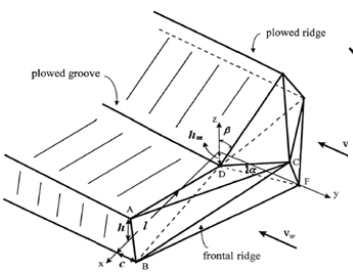

Figure2. Pluoghing with pyramidal tool (Gilormini and Felder, 1983)

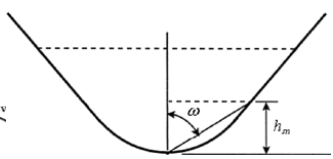

Figure 3. Rounded tip groove (gilormini and Felder, 1983)

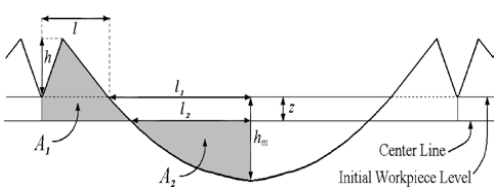

Figure 4. Shape of the scratch (Gilormini and Felder, 1983)

The tool if taken to be pyramidal and having a rounded tip as shown in the Figure 3 above then the shape of the scratch is parabolic as shown in the Figure 4 then the surface roughness can be found out from the shape of the scratch as

$$R_a = \frac{2A_1}{l+l_1} \tag{15}$$

where

$$A_1 = \frac{z}{2}(l_1 - l_2) + z\frac{tan\beta}{h} + \frac{tan\beta}{2} \tag{15a}$$

$$l = \frac{tan\beta}{h} \tag{15b}$$

$$l_1 = \sqrt{\frac{h_m}{p}} \tag{15c}$$

$$p = \frac{0.0194}{\sqrt{tan\beta}} \tag{15d}$$

The value of z can be found out by trial and error from experimentation. With the enhancement of z the surface roughness tends to worsen with grooving on the surface of the workpiece.

Surfaces except for those carefully sliced crystal surfaces tend to be rough, the roughness being a multi-scale phenomena goes down to the atomic level was shown by (Bhushan et al., 1994). Considering the importance of surface roughness in engineering, magnetic storage and instrument applications much effort has gone to characterise roughness and interaction of rough surfaces by (Thomas, 1982). Roughness has been described using fractal concepts by (Mandelbrot et al., 1984), (Majumdar and Bhushan, 1991), (Brown and Savary., 1991), (Brown et al., 1996) leading to new mathematically convenient evaluation of a variety of practical problems. While having many tools for the description of roughness, relatively less work done by (Pandit and Satyanarayanan., 1982), (Wang and Moon, 1997) has gone in to understand how surface roughness evolves as a result of natural and man-made interventions.

In grinding, the region of contact between the wheel and the workpiece consists of three characteristic zones. Cutting occurs in the leading zone, which is followed by a ploughing and then by a rubbing/sliding zone (Hahn and Lindsay, 1971; Chen and Rowe, 1996) as shown in Figure 5a. No significant amount of material is removed in the rubbing zone situated at the trailing edge and the cutting force in this zone is small. The surface roughness, which is marked in the trailing edge of

the contact zone, would thus appear to be influenced only marginally by the cutting force.

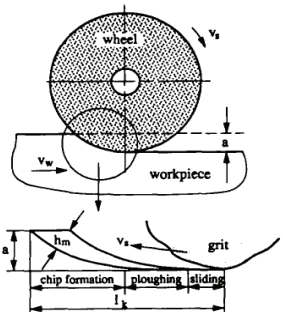

Figure 5a. Stages of chip formation (Chen and Rowe, 1996)

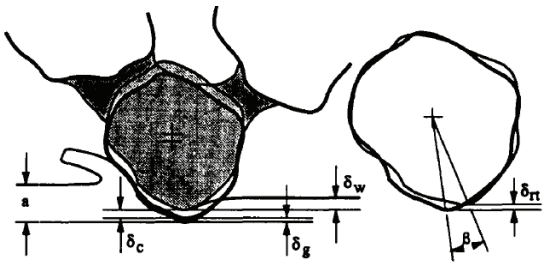

Figure 5b. Grit deflection during grinding (Saini et al., 1982)

Yossifon (1959) points out that for materials of high wear resistance the surface finish, deteriorates with increasing depth of cut as grinding is a depth-controlled process unlike lapping and polishing which are force controlled processes. Other works by (Saini et al., 1982; Li et al., 1997) suggest the relative insensitivity of surface finish to depth of cut when the depth is small. At high depths of cut the grit flakes and the heat generated at contact can cause surface damage. (Saini et al., 1982) assumed that the elastic deflection consists of four components, local workpiece deformation δ_w, grain tip deformation δ_g, variation of deflection of the grain centre δ_c and rotation δ_{rt}, as shown in Figure 5b. From their results, it was concluded that grain tip deformation δ_g and rotation δ_{rt} are relatively small. The local workpiece deformation δ_w was said to be just a little more than 2 μm and might be considered as a part of the total workpiece deflection. The deflection of the grain centre δ_c was found to be up to 3 μm. The variation of the deflection of the grain centre δ_c has a trend and scale similar to the total deflection (Saini et al., 1982). Therefore the deflection of the grain centre is considered as the local deflection in the simulation of both the dressing and the grinding process. (Nakayama et al., 1971) described the deflection of the grain centre as following the form of a Hertz distribution as

$$\delta_c = C * F_n^{0.666} \tag{16}$$

where

δ_c is expressed in micrometers
C is a constant in the range of 0.08-0.25 and 0.15 is considered an average value

F_n is the normal force acting on the grain in N

Bobji et al. (1999) presented a method to generate surface roughness based on a given roughness profile of a grinding wheel. The results pertain strictly to the first grinding pass as the wheel envelope profile changes with each subsequent pass due to fracture and blunting of abrasives as well as stock removal. Knowing the trend of wheel damage with time the envelope profile may be updated with each pass to provide the evolution of surface roughness with time.

$$S_p = \frac{h_p^2}{2ln\gamma\omega} \tag{17}$$

where S_p is the power spectra of the roughness of the sample *hp* is plastic penetration given as

$$h_p = \frac{K_{eq}}{K_p} h \tag{17a}$$

where

K_{eq} is the equivalent stiffness of abrasive-workpiece and binder-grit interfaces.
K_p is the stiffness of abrasive-workpiece
h is the global displacement (mm)
γ is a constant selected as 1.5 for phase randomisation
ω is the frequency (m^{-1})

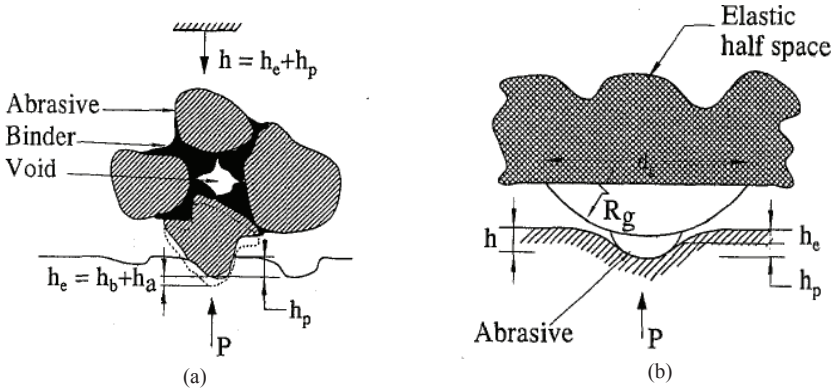

Figure 6. Illustration of abrasive-workpiece contact (Saini et al., 1982); (a) actual contact configuration and (b) model contact configuration

Figure 6 shows clearly the contact of one abrasive grain with the workpiece. Due to the contact force *P*, the grain in the binder deflects elastically by he. As grinding is a displacement controlled process, the force *P* can be determined by the total penetration h which is a sum of deflection of the wheel shaft h_w, elastic deflection of the grit-binder interface hb, elastic deflection of the grit ha, elastic deflection of the workpiece hs and plastic penetration of the workpiece hp. hw and hs are neglected as the values are small compared to hp and (hb + ha) = (he).

The roughness factor according to (Qi et al., 1997) was reduced as the effective roughness of the grinding wheel was reduced because of grinding swarf getting embedded in the pores between the active grains. The wheel wear and consequently an increase in grinding forces were observed for the same test conditions when grinding cast iron and EN9 steel. According to equation (8), smaller the roughness factor, lesser the contact length, more rubbing and an enhancement of temperature due to rubbing is observed.

Greenwood (1982) discussed the effect of load applied on rough surfaces in contact and stated that at low loads a high proportion of the contacts lie outside the Hertzian area, while at high loads the Hertz area enclosed most of the contacts between rough curved surfaces. This means that high loads diminish the effect of roughness on contact length. In grinding, wheel wear and wheel loading make the wheel dull which decreases the value of the roughness factor and increases the normal force required for removing material. The above discussed length of chip and number of cutting points and surface roughness generated will influence the mechanics involved in the generation of the ground surface.

Surface roughness as shown above is said to be affected by the elastic deformation of the wheel as it works on the workpiece during grinding, this in turn leads to the study of forces generated during the process of grinding.

5.0 FORCE MECHANICS

Hahn (1962) formulated the work and wheel removal rates as

$$Z_w = WRP_w\left(F_t - F_{t_0}\right) \quad (18)$$

$$Z_t = WRP_t\left(F_t - F_{t_0}\right) \quad (19)$$

while work removal parameters for workpiece was given by Lindsay (1971) as

$$WRP_w = \frac{7.93X10^5X\left(v_w/v_t\right)^{0.158}\left[1+\left(4a_d/3f_d\right)\right]f_d^{0.58}v_t}{d_e^{0.14}V_b^{0.47}d_g^{0.13}R_{kc}^{1.42}}p \quad m^3/sN \tag{20}$$

$$d_g = \frac{0.0254}{grain\ size}\ m \tag{20a}$$

$$V_b = 1.33H_n + 2.2S_n - 8 \tag{20b}$$

where

v_w is the workpiece surface speed, m/s
v_t is the wheel surface speed, m/s
a_d is the depth of dress, m
f_d is the feed during dressing, m
d_e is the equivalent wheel diameter, m
R_{kc} is the Rockwell hardness number of work material
V_b is the percentage volume of bond material in the wheel given by
S_n is the wheel structure number
H_n is the wheel hardness number

There have been a number of significant models developed to analyse the overall grinding forces. The most significant ones are based on the work conducted by (Hahn and Lindsay, 1971;1971a; Lindsay, 1975;1986; Hahn, 1966;1986) describe the force component to be an independent input into the grinding system from which all other parameters are determined. The work reveals that the forces generated in grinding are divided into three components: rubbing, ploughing and cutting. This is in agreement with other work by (Okumura (1967), p161) and (Busch, 1968). (Hahn and Lindsay, 1971) have experimentally determined and plotted the force and material removal relationships, linking them to the three force components as a wheel-work characteristic chart as shown in Figure 7.

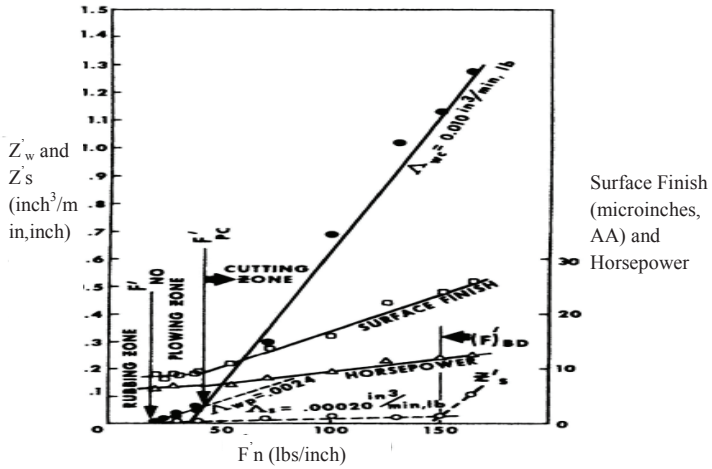

Figure 7. The Hahn and Lindsay (1971) wheel-work characteristic chart

The above graph shows the three different grinding zones of the individual force components. (Lindsay, 1986) says that the threshold force (rubbing) occurs where no material is removed below this value. The value in ploughing transition zone, both rubbing and ploughing will take place, and above this value rubbing, ploughing, and cutting will take place. If the threshold force is known, or the grinding operation has come to a steady state, a linear relationship exists between the force and stock removal rate with the slope being the work removal parameter.

The concept of the work removal parameter to determine the forces has been verified and accepted as an important grinding relationship, and has been used by numerous researchers in the field (Srinivasan, 1986; Gagliardi and Duwell, 1989; Ulrich et al., 1989; Tichy and DeVries, 1989; Cutchall, 1990).

Lindsay (1971) offers two grinding force models for the specific normal force, one for materials that are Easy-To-Grind (ETG), which are the common steels used for manufacturing, and one for materials that are more Difficult-To-Grind (DTG) such as titanium alloys, high nickel steels, M and T categories of tool steels, etc. Both models include the work removal parameter. ETG materials are commonly used for grinding applications. For ETG materials, (Hahn, 1966) has developed the following model to predict the specific normal forces during grinding

$$F_n = \frac{\pi * D_w * \overline{v_f}}{WRP} + F_{no} \tag{21}$$

where

Fn is the normal force per unit width (N)
$\underline{D_w}$ is the workpiece diameter (mm)
$\overline{v_f}$ is the in feed of wheel head (mm/sec)
WRP is the work removal parameter (mm3/s.N)
F_{no} is the threshold force (N)

As can be seen from the equation of (Hahn, 1966) normal force is made up of two components. The first is the threshold force where rubbing only occurs, and the second is for the forces developed by the material removal action of the grinding wheel. (Hahn, 1966) makes two assumptions in the equation, the wheel wear rate is negligible and grinding is done in a steady state condition, designating the workpiece deflection velocity as zero, when being ground by the grinding wheel. From experimental results the model was shown to be quite accurate to predict forces at a point of time. However, the model is not time dependent as a series of calculations are necessary to predict the forces over a length of time, due to the changing diameter of the workpiece.

Peters et al. (1974;1980) chip thickness model has also shown potential for a practical model to predict grinding forces. The equivalent chip force model is based on the thickness of a continuous layer of material being removed in the form of a chip at a volumetric rate per unit width by the grinding wheel. It has been shown that the chip thickness has a controlling influence on the forces produced in grinding (Backer et al., 1952; Reichenback et al., 1956; Snoeys and Decneut, 1971). Peters uses this parameter to develop a force grinding model as follows

$$F_n' = F_2\left(\frac{v_w a}{v_s}\right)^f = F_2\left(\frac{Q_w'}{v_s}\right)^f \tag{22}$$

where

F'_n is the specific normal force (N/mm)
F_2 is the constant (N/mm2)
v_w is the workpiece speed velocity (mm/sec)
a is the depth of cut (mm)
f is the constant

v_s is the grinding wheel speed velocity (mm/sec)
Q'_w is the volumetric removal rate per unit width (mm3/sec.mm)

The quantity within the parentheses in the above equation is the equivalent chip thickness expressed as

$$h_{eq} = \frac{v_w a}{v_s} = \frac{Q'}{v_s} \tag{23}$$

This theory relates well with the grinding forces and energy. It also associates with the other performance characteristics like surface roughness and wheel wear. However, this model has limited practical use for predicting grinding forces because the constants f and F_2 are to be determined for every particular wheel, workpiece, grinding fluid and dressing conditions, as well as on the gathered stock removal. The chip thickness model also refers to pre experimental grinding charts for characteristics of the grinding process, as shown in Figure 8. These relate the obtained equivalent chip thickness on the bottom of the chart to the predicted force or surface finish value on the left hand side of the chart or the *G* ratio of the grinding wheel on the right hand side of the chart.

The results from this approach are specific to a fairly narrow range of conditions. Changes in wheel size or type, coolant, workpiece geometry or hardness will mean that a new grinding chart is required. Since it is rather time consuming and expensive to do all the tests needed to establish a grinding chart, it is feasible to prepare them only for jobs where large numbers of similar workpieces are to be ground; even then, one grinding chart will not cover all the possible variations of the process. Both (Lindsay, 1971) and (Peters et al., 1974) models present two unique methods in predicting the forces developed by production level grinding.

Rubenstien (1972) segregated the force in grinding as chip formation force, the force component arising from the finite radius of curvature of the cutting edge, the friction force between the flank wear land and the workpiece, force for the grains to cut the workpiece, force for the grains to plough the workpiece and the friction force between the wheel bond and the workpiece material. The cutting force in grinding can simply be represented by the friction force and chip formation force by (Hahn and Lindsay, 1971). When there is no chip formation the grinding process becomes a pure friction process owing to the small normal force, the grinding process becomes a pure chip formation process at which point

there is either no friction force or the friction force is much smaller than the chip formation force which is proven by experimentation when the depth of cut is not more than 1.5 mm and equivalent diameter of grinding wheel is about 20 mm.

The normal and tangential forces for grinding in deburring process as given by (Lee et al., 1993) are

$$F_n = \frac{2K_c}{D}\left(\frac{V_w}{V_s}\right)A_w + 2K_f a_r L \quad (24)$$

$$F_t = \frac{2\varphi K_c}{D}\left(\frac{V_w}{V_s}\right)A_w + 2\mu K_f a_r L \quad (25)$$

where

a_r is the depth of cut (mm)* burr root width (mm)
L is the width of contact between the wheel and workpiece in mm
A_w is the cross sectional area of the contact zone in mm^2
D is equivalent wheel diameter
V_s is wheel speed in mm/sec
V_w is workpiece speed in mm/sec
K_c is specific chip formation force per area
K_t is specific friction force per area
μ is the coefficient of sliding friction
ϕ is the ratio of tangential chip formation force to normal chip formation force (Usuihideji, 1971) gave $\phi=\pi/(4\tan\theta_t)$ and θt is the half of the tip angle of the grains.

Malkin (1989) proposed that grinding forces can be subdivided into cutting force and sliding force, and the cutting force can further be subdivided into two more forces as chip formation force and ploughing force and as the ploughing force when compared with chip formation force is considerably less can be ignored. The forces are then composed of chip formation force and sliding force.

$$F_t = F_{t,ch} + F_{t,sl} \quad (26)$$

$$F_n = F_{n,ch} + F_{n,sl} \quad (27)$$

where

F_t is the tangential grinding force
F_n is the normal grinding force
$F_{t,ch}$ is the tangential chip formation force
$F_{n,ch}$ is the normal chip formation force

$F_{t,sl}$ is the tangential sliding force
$F_{n,sl}$ is the normal sliding force

Specific grinding energy is subdivided into specific chip formation energy and specific sliding energy, (Malkin and Cook, 1971) aggregated specific chip formation energy as

$$u_{ch} = \frac{F_{t,ch} V_s}{V_w a_p b} \tag{28}$$

where V_s is the grinding wheel velocity, V_w is the feed velocity of the work piece, a_p is the grinding depth and b is the grinding width. Taking the undeformed chip thickness and substituting in the strain rate of grinding process and further adding up with sliding force to find forces in surface grinding as given by (Tang et al., 2009) are

$$F_t = \left(K_1 + K_2 ln \frac{V_s^{1.5}}{a_p^{0.25} V_w^{0.5}}\right) \frac{V_w a_p}{V_s} b + bA \left(\alpha + \frac{4\beta p_0 V_w}{d_e V_s}\right) \left(d_e a_p\right)^{1/2} \tag{29}$$

$$F_n = \left(K_3 + K_4 ln \frac{V_s^{1.5}}{a_p^{0.25} V_w^{0.5}}\right) \frac{V_w a_p}{V_s} b + \left(\frac{4\beta p_0 V_w}{d_e V_s}\right) \left({a_p}/{d_e}\right)^{1/2} \tag{30}$$

$$K_1 = (u_s) + K_2 ln \left(\frac{k(Cr)^{0.5} d_e^{0.25}}{\gamma_0}\right) \tag{31}$$

where

u_s is specific grinding energy
K_2 is a constant to be determined by experiment, K_3=$\phi_1$$K_1$, K_4=$\phi_2$$K_2$
ϕ_1 is static normal chip formation force/static tangential chip formation force
ϕ_2 is dynamic normal chip formation force/dynamic tangential chip formation force
C is the number of active grits per unit area
r is chip width/chip thickness, d_e is equivalent diameter of wheel, V_s is wheel velocity, a_c is cutting depth, V_w is work piece velocity

The forces in surface grinding per unit width have been proposed by (Yang et al., 2011)

$$F_n' = \frac{v_w}{v_s} \left(\frac{a}{d_e}\right)^{1/2} \left[\frac{a d_e \left(k_1 + \frac{k_2 v_w}{d_e v_s}\right)}{(a d_e)^{1/2} - k_3 \frac{v_w}{v_s} a} + k_4\right] \tag{32}$$

$$F_t' = \frac{\sqrt{a d_e} \left(k_1 + \frac{k_2 v_w}{d_e v_s}\right)}{\sqrt{d_e} - k_3 \frac{v_w}{v_s} \sqrt{a}} \tag{33}$$

where

$$k_{1=}A\eta,\ k_2 = 4A\varepsilon p_0,\ k_3 = {}^{\varphi}/_{S_C N_t}\ ,\ k_4 = 4Ap_0$$

$F_n'=F_n l_s$ and $F_t'=F_t l_s$
η,ε are coefficients determined by physical and mechanical properties of contact surface
p_0 is a constant to be determined by experiment
a is the depth of cut, b is the width of grinding wheel
φ is the ratio of tangential force component to normal force component of the chip formation force

The role played by force mechanics on the quality of ground surface can be understood by contemplating how abrasion of the workpiece takes place.

6.0 ABRASION MECHANICS

The ground surface and grinding forces are affected by the surface of the wheel. The wheel should be dressed before the machined surface deteriorates beyond a quality limit of surface integrity as the deteriorated wheel will increase friction which in turn will increase the temperature at the wheel-workpiece zone. In order to achieve the best wheel surface, dressing parameters must be set. There have been a number of attempts to develop and apply mathematical models of material removal in grinding. These models use a simple energy method (Torrance, 1990; Brenner and Torrance, 1993) or slip-line field method (Black et al., 1993; Badger and Torrance, 1998) to predict cutting forces. Both can predict grinding forces approximately within 20% from wheel topography and workpiece properties. These models indicate two key parameters to be measured on the wheel: (i) the number of active grits per unit area and (ii) their attack angle as a function of depth of cut.

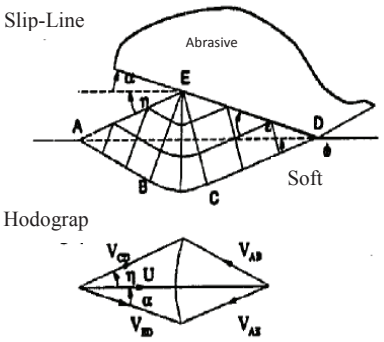

Figure 8a. Slip-line field and hodograph for rigid-plastic wave formation for mild wear (Black et al., 1993)

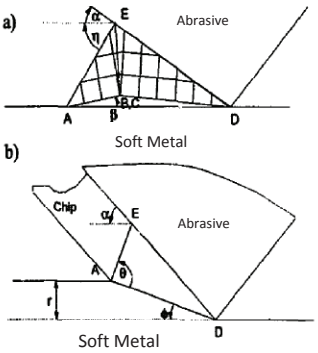

Figure 8b. Slip-line fields for (a) wedge formation and (b) cutting for severe wear (Black et al., 1993)

When the attack angle α of the abrasive is low, it will push a plastic wave ahead of it as it traverses the surface of a metal as shown in Figure 8a. (Black et al., 1993) showed that a gentle form of wear can then take place by low-cycle fatigue. Each asperity, or abrasive, on the hard surface would induce a shear strain γ in a layer of depth h as it passed over the soft surface. The value of γ depends on the attack angle, or slope, of the asperity α and the friction factor at the sliding interface (f); it can be calculated from the hodograph. The wear coefficient is formulated as

$$K = \left(\frac{n_a}{N_f}\right) h \tag{34}$$

N_f is the number of strain cycles to cause the fracture of the layer = $\left(\frac{2C}{\gamma}\right)^2$

γ is shear strain, C is the critical strain, h is the depth = $ED(sin\epsilon - sin\alpha)$, n_a is the asperities per unit length

(Kapoor, 1994) suggested that there will be a reversing of strain and this increment would produce ratchetting failure according to

$$N_f = \frac{C}{\Delta\epsilon_{xy}} \tag{35}$$

where

$\Delta_{\epsilon xy}$ is the shear strain increment which does not reverse.

Yanyi and Torrance (1997) have proved that for nonferrous materials

where unidirectional sliding is realistic the model of (Kapoor, 1994) proved to be good.

For severe wear when cutting takes place according to Figure 8a the wear coefficient is given as

$$K = \frac{\left(sin^2\alpha + \frac{1}{2}sin2\alpha\right)}{2\sqrt{3}(1+sin2\alpha)} \tag{36}$$

The force calculations according to the hodograph in Figure 8b are given as

$$F_t = \left(A\ sin\alpha + cos(2\varepsilon - \alpha)\right) \cdot ED \cdot k_s \tag{37}$$

$$F_n = \left(A\ cos\alpha + sin(2\varepsilon - \alpha)\right) \cdot ED \cdot k_s \tag{38}$$

$$\mu = \frac{F_t}{F_n} \tag{39}$$

where

$$A = 1 + {}^{\pi}/_{2} + 2\varepsilon - 2\eta - 2\alpha \tag{40}$$

k_s is the shear yield strength of the soft material

$$2\varepsilon = \arccos(f) \tag{41}$$

where

f is friction factor which is shear strength of interface/shear strength of metal

The force relationships and equivalent chip thickness according to (Torrance, Buckley, 1996) with l_a as the length of the arc of cut and σ_y as the yield strength of the work piece are

$$F_n' = P_n . b_a . l_a \tag{42}$$

$$F_t' = P_t . b_a . l_a \tag{43}$$

$$h_{eq} = \frac{KF_n'}{\sigma_y} \tag{44}$$

where

b_a is the fraction of the wheel surface in contact with the work piece
p is the average contact pressure over the arc of cut as Pn*ba
μ is the summation of the slope of friction

$$\alpha \text{ as } \frac{F_t}{F_n} = \frac{P_t}{P_n} = \sum \mu_\alpha \cdot P_\alpha \cdot \delta\alpha \tag{44a}$$

$$K \text{ is the overall wear coefficient} = \sum K_\alpha \cdot P_\alpha \cdot \delta\alpha \tag{44b}$$

A two-body abrasive wear model was presented by (Zum Gahr, 1988) of abrasive particles harder than the wearing material. He proposed the mechanisms in which the abrasive particles will interact with the workpiece as shown in Figure 9(a).

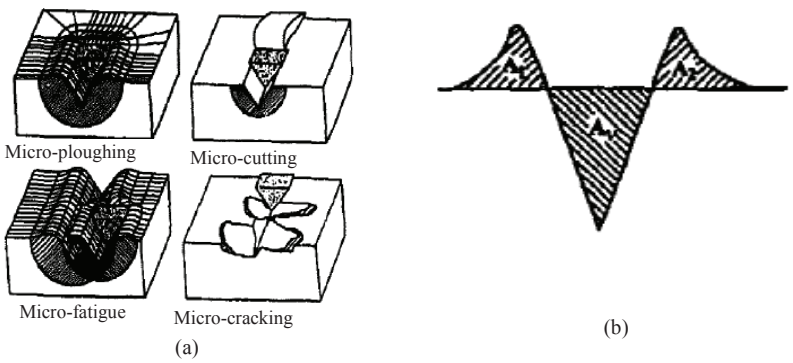

Figure 9. (a) Interaction between abrasive particles and the wearing surface (Zum Gahr, 1988) and (b) Cross-section through a wear groove produced by a sliding abrasive particle, defining the areas used for calculating f_{ab} (Zum Gahr, 1988)

$$f_{ab} = \frac{A_V - (A_1 + A_2)}{A_V} \tag{45}$$

where

f_{ab} is the amount of volume loss with respect to the volume of the wear groove as a result of the four above illustrated abrasive wear processes
A_V is the cross-sectional area of the wear groove
A_1 and A_2 is the amount of material pushed to each side by plastic deformation

When f_{ab} = 0, ideal micro-ploughing (zero wear) happens, whereas f_{ab} = 1, ideal micro-cutting with the worn volume directly proportional to

the cross-sectional area of the wear groove. Linear wear intensity $W_{1/s}$ was formulated as

$$W_{1/s} = \varphi_1 * f_{ab} * \frac{p}{H_{def}} \tag{46}$$

where ϕ_1 is the shape factor dependent on the geometry of the abrasive particle, p is the applied surface pressure, H_{def} is the hardness of the wear debris. (Zum Gahr, 1988) corroborated the fact that increased f_{ab} values resulted in increased occurrence of micro-cutting by experimental data.

Abrasion mechanics paved a way for the finding the way in which cutting can happen instead of ploughing and wedge formation and this along with the formulation of fracture toughness of the workpiece leads to finding the method in which we can grind a given workpiece to a certain surface finish.

7.0 FRACTURE TOUGHNESS

Moore and King (1979) cited that the rate of material removal and the wear process is determined by applied load, material hardness and ratio of fracture toughness to material hardness. The ratio is low for higher loads and the wear rate was high and the debris was formed by fracture. Figure 10(a) below shows the relationship between a material's fracture toughness and wear resistance under abrasive conditions. (Gahr, 1978) reported that abrasive particles initiated both micro-ploughing and crack propagation of the wearing material only when the exerted load was above the critical value given by P_{crit}. Further fracture toughness of the material influenced the critical load and hence the wear resistance.

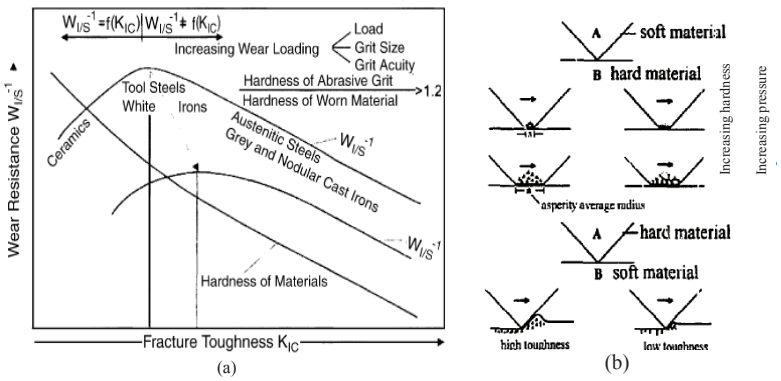

Figure 10. (a) Wear resistance and fracture toughness for ceramics and metals (Zum Gahr, 1978) and (b) Asperity deformation for materials of different toughness and applied pressures (Hornbogen, 1975)

Hornbogen (1975) proposed a model that related increased wear rates to decreasing fracture toughness of materials as shown in Figure 10(b). The model was based on the concept of strain that happened during asperity interaction ($\varepsilon_{d'eff}$) and the critical strain at which crack growth was initiated ($\varepsilon_{c'eff}$). Range I wear regime was said to be when applied strain was smaller than critical strain then wear rate was independent of fracture toughness and wear coefficient was constant and wear resistance increased proportionally with hardness. Range II was the one where the applied strain was larger than the critical strain of the material and the probability of crack growth was enhanced, which led to higher wear rate. The wear rate relation was given for Range II materials as

$$W = K_0 \frac{\varepsilon_{d,eff} * P}{\varepsilon_{c,eff} * H} \tag{47}$$

where

K_0 is the wear coefficient, defined as the probability of wear particle formation $\varepsilon_{d'eff}$ is strain at asperities undergoing plastic deformation $\varepsilon_{c'eff}$ is the strain associated with crack growth within asperities
P is the applied pressure
H is the material hardness

This model was on the assumption that crack growth determined the wear behaviour in the Range II regime and assumed that in Range I in addition to plastic deformation of asperities, sub-critical crack growth was active.

Studies on fracture, using plastic indentation to determine fracture toughness of brittle materials were done and the relationship for fracture toughness K_{IC} of brittle materials was given by (Evans., Charles, 1976)

$$K_{IC} = 0.05 * H\sqrt{a} * k\left(\frac{C}{a}\right)^{-1.5} \tag{48}$$

where

H is hardness
C is crack length produced by indentation
a is the radius of indentation
k is the correction factor=3.2 for $\frac{C}{a} \geq 3$

Kakaba et al. (1981) reported that in a single pass of sliding of an abrasive asperity on a metallic surface, three wear modes were noted as cutting, wedge formation and ploughing. (Kato, 1992) said that the grove formation on the wearing surface resulted from the micro-hardness of the asperity and its attack angle. It was found that wear particle shape, size, structure and number could be determined by understanding the microscopic wear mode which is controlled by the microscopic fracture mode. Degree of penetration D_p of an asperity was included to relate the three-dimensional severity of contact for wear and was given as

$$D_p = \frac{h}{a} = R\left(\frac{\pi H}{2W}\right)^{0.5} - \left(\frac{\pi R^2 H}{2W} - 1\right)^{0.5} \quad (49)$$

where

a is the contact radius
h is depth of penetration
R is radius of spherical asperity
H is hardness of the indented surface
W is the load applied

The relative shear strength parameter, *f* was defined as the ratio of shear strength of the interface to the bulk material and was used to relate frictional condition at the abrasive particle surface interface and graphically shown in Figure 11. This parameter was possible because of the research by (Challen and Oxley, 1979).

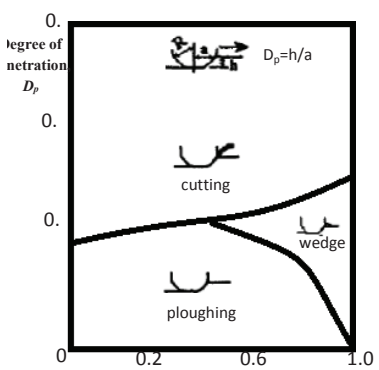

Figure 11. Abrasive wear mode diagram for metals (Kato, 1992)

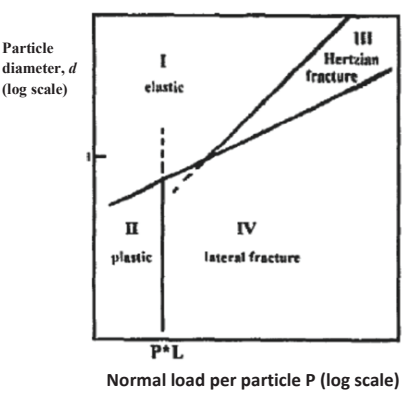

Figure 12. Plot showing the wear regimes for an abrading surface, over which abrasive particles cause plastic flow or fracture in the material. *P* L* indicates the transition related to lateral fracture (Hutchings, 1992)

(Hutchings, 1992) suggested that for abrasive wear a transition occurred from brittle, fracture-dominated behaviour to plastic-dominated

behaviour for hard second-phase particles in wearing microstructure as abrasive particle size reduced. The main fracture modes were considered to be Hertzian cracking and lateral fracture showing the importance of fracture toughness in the finding of this transition. Lawn and Marshall (1978) derived an expression for the threshold abrasive particle size, d_{OH} which was defined as the value above which Hertzian fracture occurred rather than plastic flow as

$$d_{OH}\ \alpha\ \left(\frac{K_{ct}}{H_I}\right)^2 \frac{E}{H_I} \tag{50}$$

where

K_{ct} is fracture toughness of the wearing material
H_I is indentation hardness of the wearing material
E is young's modulus of the wearing material

(Hutchings, 1992) developed a graph as shown in Figure 12 describing the mode of failure for these hard second-phase particles as a function of abrasive grit size, and of the load these particle exerted on the second phase particles in the microstructure.

This shows that the threshold particle size of the grain can be found out by knowing the fracture toughness, indentation hardness and young's modulus of the workpiece which is brittle in nature, by which we can find out what can be the variety of wheel we can use to get the required surface roughness to the workpiece.

8.0 CONCLUSIONS

The length of chip varies depending on dry or wet process, hardness of material, depth of cut, wheel speed, workpiece speed, angle of attack and thickness of chip is also dependent on the workpiece and wheel speeds, size and shape of grains, dry or wet process, fracture toughness of materials.

The size and shape of the grains will decide the amount of material to be removed and the chip thickness will influence the specific energy required and this will affect the process of grinding on a whole. The size of the grains if smaller or having more gaps between successive grains has the possibility of accumulating swarf thereby reducing the depth of cut and grinding capability and enhance rubbing. The size of the

abrasive grain in the wheel has to be decided on the fracture toughness and hardness of the workpiece being ground, this leads to the question can a universal abrasive be used to ground all sorts of materials or a specific abrasive has to be experimented and the required size of grit found for each of the workpiece.

The size of the grain, depth of cut, hardness of wheel and workpiece will affect the finish attained of the workpiece. The knowledge of the grit included angle and the depth of cut an estimation of surface roughness can be had. When the roughness factor reduces the length of the contact of the wheel and workpiece reduces increasing the force required to cut the workpiece and the necessity of dressing is enhanced as a loss in surface finish becomes visible and there is an increase in temperature due to rubbing.

Forces induced in the wearing material due to the action of the abrasives across the workpiece are occurring due to two actions of the abrasive grains against the workpiece namely cutting and sliding. The sliding component tends to reduce when the wheel has a good roughness factor and is dressed properly thereby reducing the force being exerted on the workpiece during machining.

Modelling of two-body abrasive wear again emphasizes the influence of the wearing materials workhardening ability, fracture toughness and hardness on the wear mechanism. For ductile materials subjected to abrasive wear, microploughing is the most favoured mechanism, resulting in a low wear rate, Brittle materials usually exhibit one of the following wear mechanisms: micro-cutting; microfatigue or microcracking.

The analysis of the size of grit and the bond material of grinding wheels used to grind different workpieces have to be researched, and a suitable combination has to be hammered out to get the best surface finish and less force induced stresses on the workpiece.

REFERENCES

Abebe, M. and Appl, F. C. (1988). Theoretical analysis of the basic mechanics of abrasive processes: Part I. General model. *Wear, 126*, 251-266.

Azarkhin, A., Richmond, O. and Devenpeck, M. (1996). An approximate model of surface ploughing by a rotating disc and other indenters. *Wear, 192,* 157-164.

Backer, W. R., Marshall, E. R. and Shaw, M.C. (1952). The size effect in metal cutting. *Transactions of ASME*, 61-72.

Badger, J. A. and Torrance, A. A. (1998). A computer program to predict grinding forces from wheel surface profiles using slip-line fields. In P*roceedings of the Conference in Advanced Manufacturing Technologies*, San Sebastian.

Bhushan, B., Koinkar, V. N. and Ruan, J. A. (1994). Micro tribology of ground media. *Proceedings of Institution of Mechanical Engineers,* Part J, 208(1), 17-29.

Black, A. J., Kopalinsky, E. M. and Oxley, P. L. B. (1993). Asperity deformation models for explaining the mechanisms involved in friction and wear. *Proc. I. Mech. E.*, 207, 335-353.

Bobji, M. S., Venkatesh, K. and Biswas, S. K. (1999). Roughness generated in surface grinding of metals. *Journal of Tribology, 121*, 746-752.

Brecker, J. N. and Shaw, M. C. (1974). Measurement of the effective number of cutting points in the surface of a grinding wheel. *In Proceedings of the International Conference on Production Engineering* (pp. 740-745). Tokyo, Japan: Japan Society of Precision Engineers.

Brenner, N. and Torrance, A. A. (1993). Wheel sharpness measurement for force prediction in grinding. *Wear, 160*, 317-323.

Brown, C. A. and Savary, G. (1991). Describing ground surface texture using contact profilometry and fractal analysis. *Wear, 141*, 211-226.

Brown, C. A., Johnsen, W. A. and Butland, R. M. (1996). Scale-sensitive fractal analysis of turned surfaces. *Annals of CIRP, 45(*1), 515-518.

Brown, R. H. and Watson, J. D. (1977). An examination of the wheel-work interface using an explosive device to suddenly interrupt the surface grinding processes. *General Assembly of CIRP*, pp. 43.

Busch, D. M. (1968). Ritz und verschleissuntersuchungen an sproden werkstoffen mit einzelkornbestuckten hartstoffwerkzeugen, *Technische Hochschule: Hannove*r, West Germany.

Challen J. M. and Oxley, P. L. B. (1979). An explanation of the different regimes of friction and wear using asperity deformation models. *Wear, 53,* 229-243.

Chen, X. and Rowe, W. B. (1996). Analysis and simulation of the grinding process, Part II: Mechanics of Grinding. *International Journal of Machine Tools and Manufacturing, 36*(8), 883-896.

Cutchall, D. Z. (1990). Optimization of the cam grinding process. Technical paper, *Society of Manufacturing Engineer*s, MR90 -510 -1 to MR90- 510-11.

Evans, A. G. and Wilshaw, T. R. (1976). Quasi-static solid particle damage in brittle solids. *Acta Met., 24*, 939-956.

Evans A. G. and Charles, E. A. (1976). Fracture toughness determination by indentation. J. Am. *Ceram. Soc*., 59, 371-378.

Gagliardi, J. J. and Duwell, E. J. (1989). Mechanisms of grinding using coated abrasives made with abrasive grit clusters. *Mechanics of Deburring and Surface Finishing Processes, 38*, 107-122.

Gilormini, P. and Felder, E. (1983). Theoretical and experimental study of the plowing of a rigid-plastic semi-infinite body by a rigid pyramidal indenter. *Wear, 88*, 195-206.

Greenwood J. A. (1982). T*he contact of real surfaces, contact mechanics and wear of rail/wheel system*, University of Waterloo Press, pp. 21-35.

Hahn, R. S. (1966). On the mechanics of the grinding process under plunge cut conditions. *Transactions of ASME*, 72-80.

Hahn, R. S. (1986). Precision grinding cycles. R.I.H. King. et al. (Eds.), *Handbook of modern grinding technology*, (pp. 170-190) New York, London: Chapman and Hall.

Hahn, Robert. S., Lindsay, Richard. P. (1971). Principles of grinding: theory, techniques and troubleshooting, C.L. Bhateja. et al. (Eds.), Society of Manufacturing Engineers: Dearborn, Michigan. pp. 3-41.

Hahn, R. S. (1962). On the nature of the grinding process, In *Proceedings of the Third International Conference on Machine Tool Design and Research*, September 1962 (pp.129-164). Birmingham: Pergamon Press.

Hornbogen, E. (1975). The role of fracture toughness in the wear of metals. *Wear, 33*, 251-259.

Hutchings, I. M. (1992). Ductile-brittle transitions and wear maps for erosion and abrasion of brittle materials. *J. Phys. D, 25*, A212-A221.

Hwang, T. W. and Malkin, S. (1999). Upper bound analysis for specific energy in grinding of ceramics. *Wear, 231*, 161–171.

Kapoor, A. (1994). A re-evaluation of the life to rupture of ductile metals by cyclic plastic strain. *Fatigue Fract. Eng. Mater. Struct, 17*, 201-219.

Kate, K. (1992). Micro-mechanisms of wear-wear modes. *Wear, 153*, 277-295.

Kayaba, T., Kato, K. and Nagasawa, Y. (1981). Abrasive wear in stick-slip motion. In *Proc. Int. Conf. on Wear of Materials*, (pp. 439-446) San Francisco, California, USA: *ASME*, New York.

Lee, K. C., Huang, H. P. and Lu, S. S. (1993). Burr detection by using vision image. *International Journal of Advanced Manufacturing Technology, 8*, 275-284.

Lawn and Marshall, D. B. (1978). *Fracture mechanics of ceramics*, Vol. 3, Flaws and Testing, Plenum Press, New York.

Li, K., Liao, T. W., O'Rouke, L. J. and McSpudden, Jr., S. B. (1997). Wear of diamond wheels in creep-feed grinding of ceramic materials: effects on process response and strength. *Wear, 211*, 104-112.

Lindsay, R. P. (1971). *On the material removal - and wheel removal parameters - Surface finish, geometry and thermal damage in precision grinding*. (PhD thesis), Worchester Polytechnic Institute, USA.

Lindsay, R. P. (1986). Principles of grinding, R.I.H. King. et al. (Eds.). *Handbook of modern grinding technology*, (pp. 30-71) New York, London: Chapman and Hall.

Lindsay, R. P. and Hahn, R.S. (1971). On the basic relationships between grinding parameters. Annals of the CIRP, XVIV, 657-666.

Lindsay, Richard. P. (1975). Principles of grinding: four years later grinding: Theory, techniques and troubleshooting, (pp. 42-60) Dearborn, Michigan: Society of Manufacturing Engineers.

Mahdi, M. A. and Zhang, L.C. (1999). Applied mechanics in grinding. Part 7: Residual stresses induced by the full coupling of mechanical deformation, thermal deformation and phase transformation. *International Journal of Machine Tools and Manufacture, 39*(8), 1285-1298.

Majumdar, A., Bhushan, B. (1991). Fractal model of elastic-plastic contact between rough Surfaces. *ASME Journal of Tribology, 113*, 1-11.

Makino, H., Suto T. and Fukushima E. (1966). An experimental investigation of the grinding process. *J. Mech. Lab. Japan, 12*(1), 17-21.

Malkin, S. (1989). *Grinding Technology theory and applications of machining with abrasives*, Dearborn, Michigan: Society of Manufacturing Engineers.

Malkin, S. and Cook, N. H. (1971). The wear of grinding wheels, Part 1: Attritious wear. Transactions of ASME. *Journal of Engineering for Industry, 93*, 1120-1133.

Mandelbrot, B. B., Pescoja, D. E. and Paullay, A. J. (1984). Fractal Character of fracture surface of metals. *Nature, 308*, 721-722.

Maris, M. (1977). *Thermische aspekten van de oppervlakteintegriteit bij het slijpen*. (PhD thesis). Katholieke Universiteit te Leuven, Belgien.

Moore, M. and King, F. (1979). Abrasive wear of brittle solids. *Proc Intl Conf Wear Materials ASME*, 275-284.

Nakayama, K., Brecker, J. and Shaw, M. C. (1971). Grinding wheel elasticity. Trans. *ASME J. Engng Industry, 93*(5), 609-614.

Okamura, K. (1967). Study on the cutting mechanism of abrasive grain (4th Report). Bull. *Japan Soc. of Prec. Eng., 33(*3), 161.

Pandit, S. M. and Satyanarayanan, G. (1982). A Model for surface grinding based on abrasive geometry and elasticity. *ASME Journal of Engineering for Industry, 104*, 349-357.

Peters, J. and Aerens, R. (1980). Optimization procedure of three phase grinding cycles of a series without intermediate dressing. *Annals of the CIRP, 29*(1), 195-200.

Qi, H. S. (1995). *A contact length model for grinding wheel-workpiece contact*. (PhD thesis). Liverpool John Moores University, UK.

Qi, H. S., Rowe, W. B. and Mills, B. (1997). Experimental investigation of contact behaviour in grinding. *Tribology International, 30*(4), 283-294.

Qi, H. S., Mills B. and Rowe W. B. (1994). An analysis of real contact length in abrasive machining processes using contact mechanics. *Wear, 176*, 137-141.

Reichenbach, G. S., Mayer, I. E., Kalpakcioglu, S. and Shaw, M. C. (1956). The role of chip thickness in grinding. *Transactions of ASME, 18,* 847- 850.

Rowe, W. B., Qi, H. S., Morgan M. N. and Zheng H. W. (1993). The effect of deformation on the contact area in grinding. *Annals of CIRP, 42*(1), 409-412.

Rowe, W. B., Qi, H. S., Morgan M. N. and Zheng H. W. (1993a). The real contact length in grinding based on depth of cut and contact deflections. In *Proc. Thirtieth International MATADOR Conference* (pp.187-193), UMIST, Macmillan.

Rubenstein, C. (1972). The mechanics of grinding. *International Journal of Machine Tool Design and Research, 12*, 127-139.

Saini, D. P., Wager, J. G., and Brown, R. H. (1982). Practical significance of contact deflection in grinding. *Annals of CIRP, 31*(1), 215-219.

Shaw, M. (1972). Fundamentals of grinding. Proceeding of the International Grinding Conference: New Developments in Grinding (pp. 221-258), Pittsburgh, Pennsylvania.

Shaw, M. C., Farmer, D. A. and Nakayama, K. (1967). Mechanics of the abrasive cut-off operation. Trans. *ASME J. Eng. Ind., 89*, 495-502.

Snoeys, R. and Decneut, A. (1971). Review of results of the co-operative research program of the CIRP grinding group. *Annals of the CIRP, 19*, 507-512.

Snoeys, R., Peters, J., Inst., V. W. and Decneut, A. (1974). The significance of chip thickness in grinding, *Annals of the CIRP, 23*(2), 227-237.

Srinivasan, K. (1986). *Grinding chatter and vibrations*, R.I.H. King. et al (Eds.) Handbook of modern grinding technology. Chapman and Hall: New York, London. pp. 119 - 169.

Suh, N. P. (1986). *Tribophysics*. Prentice-Hall, Englewood Cliffs, NJ, Chap. 7.

Tang, J., Du, J. and Chen, Y. (2009). Modeling and experimental study of grinding forces in surface grinding. *Journal of Materials Processing Technology, 209,* 2847-2854.

Thomas, T. R. (1982). *Rough Surfaces*, Longman, London.

Tichy, J., DeVries, W. (1989). *A model for cylindrical grinding based on abrasive wear theory*. S.K. Malkin. (Eds.) Grinding Fundamentals and Applications, The American Society of Mechanical Engineers: San Francisco, California. pp. 335-348.

Torrance, A. A. (1987). An approximate model of abrasive cutting. *Wear, 118*, 217–232.

Torrance, A. A. and Buckley, T. R. (1996). A slip line field model of abrasive wear. *Wear, 196*, 35–45.

Torrance, A. A. (1990). The correlation of process parameters in grinding. *Wear, 139*, 383–401.

Ulrich, B. J., Srivastava, A. K., Elbestawi, M. A. and Veldhuis, S. (1989). *Force modelling of the robotic disk grinding process*, S.K. Malkin. (Eds.) Grinding Fundamentals and Applications. The American Society of Mechanical Engineers: San Francisco, California. pp. 105-130.

Usuihideji. (1971). T*echnology of Cutting and Grinding*, Japan.

Vathaire, M. D., Delamare, F. and Felder, E. (1981). An upper bound model of plowing by a pyramidal indenter. *Wear, 66*, 55-64.

Verkerk, J. (1975). The real contact length in cylindrical plough grinding. *Annals of CIRP, 24*, 259.

Wang, Y., Moon, K. S. (1997). A Methodology for the multi resolution simulation of grinding wheel surface. *Wear, 211*, 218-225.

Yang, H., Zhang, L., Li, D. and Li, T. (2011). Modeling and analysis of grinding force in surface grinding. In Computer Science and Automation Engineering (CSAE), 2011 *IEEE International Conference* (Vol. 2, pp. 175-178).

Yang, Y. and Torrance, A. A. (1997). Wear by plastic ratchetting: An experimental evaluation, *Wear, 196*(1-2), 147-155.

Yossifon, S. (1982). The surface roughness produced when austenitic stainless steel is ground by Alumina Wheels. *Annals of the CIRP, 31*, 225-228.

Zhen Bing Hou, Ranga Komanduri. (2003). On the mechanics of the grinding

process – Part I Stochastic nature of the grinding process. *International Journal of Machine Tools and Manufacture, 43*, 1579–1593.

Zhang, L. C., Suto, T., Noguchi, H. and Waida, T. (1993). Applied mechanics in grinding part II: Modelling of elastic modulus of wheels and interface forces. *International Journal of Machine Tools and Manufacture, 33*(2), 245-255.

Zhang, L. C., Suto, T., Noguchi, H. and Waida, T. (1993). Applied mechanics in grinding-III. A new formula for contact length prediction and a comparison of available models. *International Journal of Machine Tools and Manufacture, 33*(4), 587-597.

Zum Gahr, K. H. et al. (Eds.) (1997). Wear by hard particles. New Directions in Tribology, Institute of Mechanical Engineers, London.

Zum Gahr, K. H. (1988). Modelling of two-body abrasive wear. *Wear, 124*(1), 87-103.

Zum Gahr, K. H. (1978). Relation between abrasive wear rate and the fracture toughness of metallic materials. *Z.Metallkde, 69*, 643-650.